JOURNAL OF MATERIALS SCIENCE 23 (1988) 3026–3030

Properties of indium oxide/tin oxide multilayered films prepared by ion-beam sputtering

TAKEYUKI SUZUKI, TSUTOMU YAMAZAKI, HARUNOBU ODA
Department of Industrial Chemistry, Faculty of Technology, Tokyo University of Agriculture and Technology, Koganei, Tokyo 184, Japan

The preparation and characterization of indium oxide (InO_x)/tin oxide (SnO_y) multilayered films deposited by ion-beam sputtering are described and compared with indium tin oxide (ITO) films. The structure and the optoelectrical properties of the films are studied in relation to the layered structures and the post-deposition annealing. Low-angle X-ray diffraction analysis showed that most films retained the regular layered structures even after annealing at 500° C for 16 h. As an example, we obtained a resistivity of $6 \times 10^{-4}\,\Omega$ cm and a transparency of about 85% in the visible range at a thickness of 110 nm in a multilayered film of InO_x (2.0 nm)/SnO_y (0.2 nm) × 50 pairs when annealed at 300° C for 0.5 h in air. Hall coefficient measurements showed that this film had a mobility of 17 $cm^2\,V^{-1}\,sec^{-1}$ and a carrier concentration (electron density) of $5 \times 10^{20}\,cm^{-3}$.

1. Introduction

Optically transparent and electrically conducting films based on indium tin oxide (ITO) have been extensively studied as transparent electrodes and as heat-reflecting filters for energy-saving purposes. Efforts have been made to improve the optoelectrical properties of ITO films for higher transmissivity in the visible spectral region, higher reflectance in the IR region and higher electrical conductivity. However, all of these investigations were carried out on films of ITO solid solutions. It is obvious from review papers [1, 2] that the properties of ITO films depend largely on the preparation method. Here we propose a new approach to study ITO films, starting from multilayered films composed of repeated alternate deposition of ultrathin layers of indium oxide (InO_x) and tin oxide (SnO_y). This paper deals with the fabrication and properties of InO_x/SnO_y multilayered films and the effects of post-deposition heat treatment on the structure and properties of these films.

2. Experimental methods

Multilayered films of InO_x/SnO_y were prepared using an ion-beam sputtering (IBS) apparatus. The central part of the IBS apparatus is shown schematically in Fig. 1. An argon ion-beam of 1000 V and 0.8 mA hits the In_2O_3 (99.99% pure) and SnO_2 (99.99% pure) targets alternately and thus deposits the multilayered films on a fused quartz substrate. Each layer thickness is controlled by the sputtering time by rotating the targets with a stepping motor via a microcomputer and a driver/controller. The substrate temperature is lower than 90° C and the chamber pressure during the run is maintained at 1×10^{-4} torr. Details of the IBS apparatus have been published elsewhere [3, 4]. The thickness and thus the rate of deposition of a pure film were measured with a surface texture measuring instrument. The layer repeat length and the total thickness of the multilayered films were also measured from a low-angle X-ray diffraction pattern. X-ray diffraction was carried out with 30 kV, 20 mA Cu$K\alpha$ radiation (RAD-B, Rigaku). The diffractometer scans for the low-angle X-ray were taken using a 0.5° divergence slit and a 0.15 mm receiving slit. The intensity data were collected with a scan speed of 0.2° min^{-1} and a step sampling of 0.002° in 2θ. The transmissivity was measured using a double-beam spectrophotometer (Hitachi-228). The electrical properties were obtained by the Van der Pauw technique at room temperature. Hall effect data were taken in a d.c. magnetic field of 5500 G (0.55 T). The post-deposition annealing was carried out in an electric furnace in air.

3. Results and discussion

3.1. Structure

Four kinds of InO_x/SnO_y multilayered films with nearly the same total thickness were prepared. Actually the total thickness, as measured from the low-angle X-ray diffraction, varied from 110 to 114 nm. The thickness of InO_x and SnO_y in a layer repeat length (pair thickness) and the number of pairs are shown in Table I.

TABLE I Preparations of InO_x/SnO_y multilayered films

Film designation	Pair thickness InO_x (nm)/SnO_y (nm)	Number of pairs
(a)	1.0/0.1	100
(b)	2.0/0.2	50
(c)	5.1/0.6	20
(d)	10.2/1.2	10

0022–2461/88 $03.00 + .12

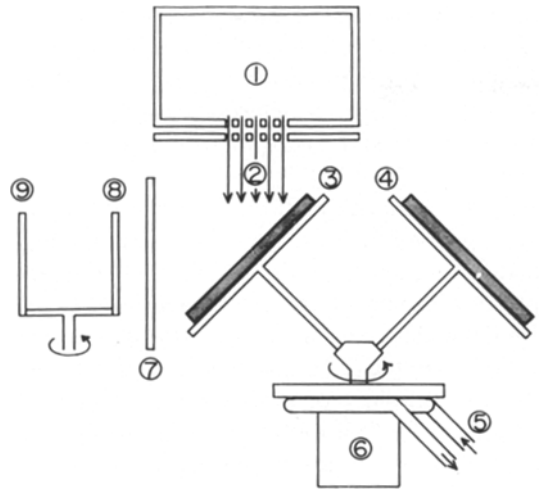

Figure 1 Schematic illustration of the central part of the ion-beam sputtering apparatus. Multilayered films are deposited by sputtering the two targets A and B. (1) Ion source, (2) ion-beam, (3) Target A, (4) Target B, (5) water inlet and outlet, (6) stepping motor, (7) shutter, (8) Substrate A, (9) Substrate B.

The pair thickness is designed using the deposition rate of 0.018 nm sec^{-1} for InO_x and 0.042 nm sec^{-1} for SnO_y. The pair thickness is actually determined from the low-angle X-ray diffraction.

The designed values are in good agreement with the experimental ones for Films (b), (c) and (d); however, Film (a) showed no low-angle diffraction peaks. As-deposited Films (c) and (d) were amorphous as revealed from the ordinary higher-angle X-ray diffraction analysis, while Films (a) and (b) showed traces of broad crystalline peaks of the (2 2 2) and (4 0 0) planes of cubic In_2O_3 (JCPDS 6-0416). The formation of dense interfaces between the ultrathin InO_x and SnO_y is probably responsible for these small peaks. It is interesting that this structural ordering at the dense interfaces can be observed at substrate temperatures lower than 90° C. The effects of post-deposition annealing on the structure of these multilayered films were also examined; films were annealed at 300° C for 0.5 h, 300° C for 5 h and 500° C for 16 h. Many processes such as absorption of oxygen, diffusion of the constituent atoms and crystallization are involved in the annealing of these multilayered films.

We now look at the overall effects of annealing on the structure of the multilayered films. Typical examples of Film (c) are given in Figs 2 and 3. Fig. 2 shows the low-angle X-ray diffraction patterns. Diffraction peaks are observed at the diffraction angle θ from the nth reflection which satisfies Bragg's equation, $2d \sin \theta = n\lambda$, where d is the layer repeat length (pair thickness) and λ is the wavelength of the X-rays (0.154 nm). An analysis of this figure shows that post-deposition annealing decreases the layer repeat length d; it changed from 5.66 ± 0.04 nm for as-deposited films to 5.56 ± 0.01 nm for the films annealed at 500° C for 16 h. Contrary to our expectation, annealing at 300° C greatly increased the intensity from the $n = 1$ and 2 relections. It is rather surprising that the second-order reflection can be clearly observed after an anealing at 500° C for 16 h; a strong periodic nature along the thickness still exists.

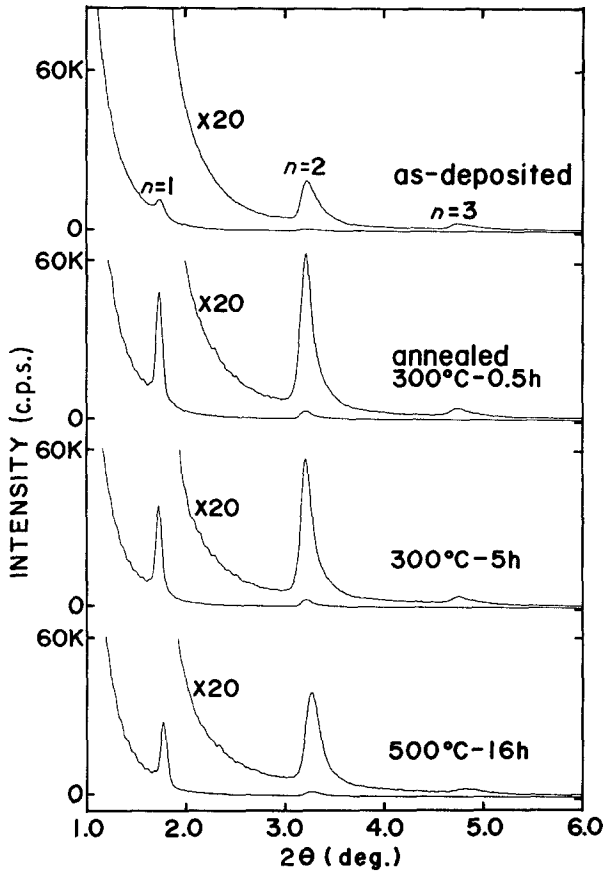

Figure 2 Low-angle X-ray diffraction patterns of the multilayered Film (c) (Table I). Annealing at 300° C increased the intensity from the $n = 1$ and 2 reflections.

A longer annealing at higher temperatures is needed to form a homogeneous ITO solid solution from the multilayered films. Detailed analysis of the residual periodic nature after annealing is in progress. Fig. 3 is

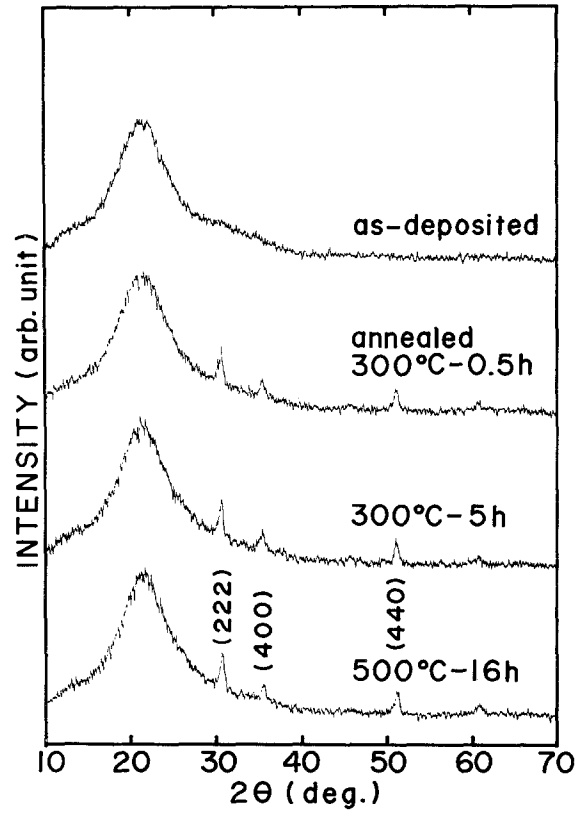

Figure 3 High-angle X-ray diffraction patterns of the multilayered Film (c).

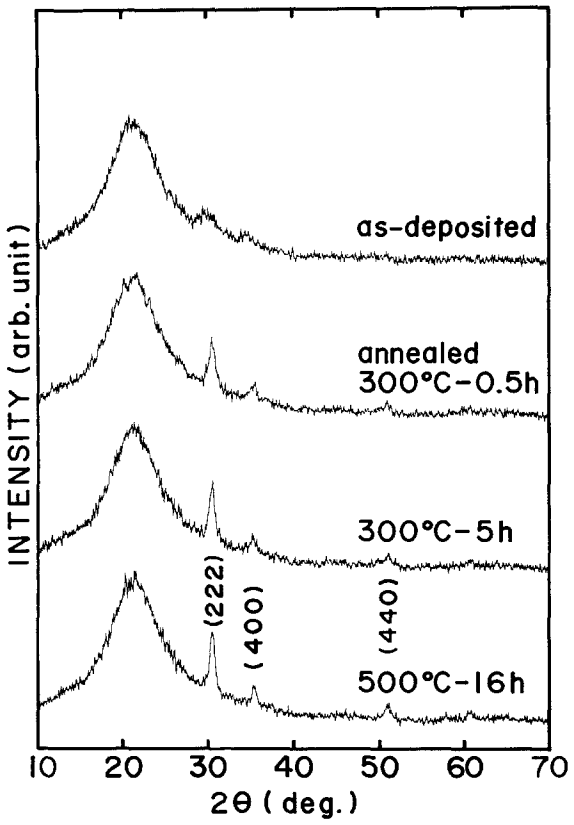

Figure 4 High-angle X-ray diffraction patterns of the multilayered Film (a).

the ordinary high-angle X-ray analysis of Film (c). The as-deposited multilayer is amorphous. It is noted that the first annealing at 300° C for 0.5 h greatly enhances the growth of the (2 2 2), (4 0 0) and (4 4 0) planes and that the subsequent annealings do not increase the intensity of these lines so much. Fig. 3 shows that the cubic In_2O_3 solid solution grows on the substrate without preferred orientation. However, these solid solutions are heterogeneous, since a strong periodic nature still exists in the annealed films as shown in Fig. 2.

Fig . 4 shows the high-angle X-ray diffraction of Film (a) which has the shortest layer repeat length. In Film (a), the intensity of the diffraction lines gradually increases with annealing. A comparison of the Figs 3 and 4 demonstrates that the growth of the strongest reflection from the (2 2 2) plane is promoted by annealing for the multilayered films made of thinner layers. Solid-solution formation through diffusion in multilayered films is an interesting subject and will be treated in a separate paper.

3.2. Optical properties

The optical properties were studied by measuring the transmissivity between 200 and 900 nm. Fig. 5 shows the results for as-deposited films. Film (d) keeps the highest transmissivity T at almost all the wavelengths measured; the highest T ($> 90\%$) is observed at about 440 nm. The other three films behave differently from Film (d). They generally show lower visible transmissivity (T = 80 to 85%); it is worth noting that Films (a) and (b) exhibit a slightly higher T than that of Film (d) around 310 nm.

The change of transmissivity on annealing is given in Fig. 6. Here is shown only the curves for Films (a) and (d), because the behaviour of Film (a) nearly represents that of Films (b) and (c) and the transmissivity of Film (d) remains almost constant throughout the

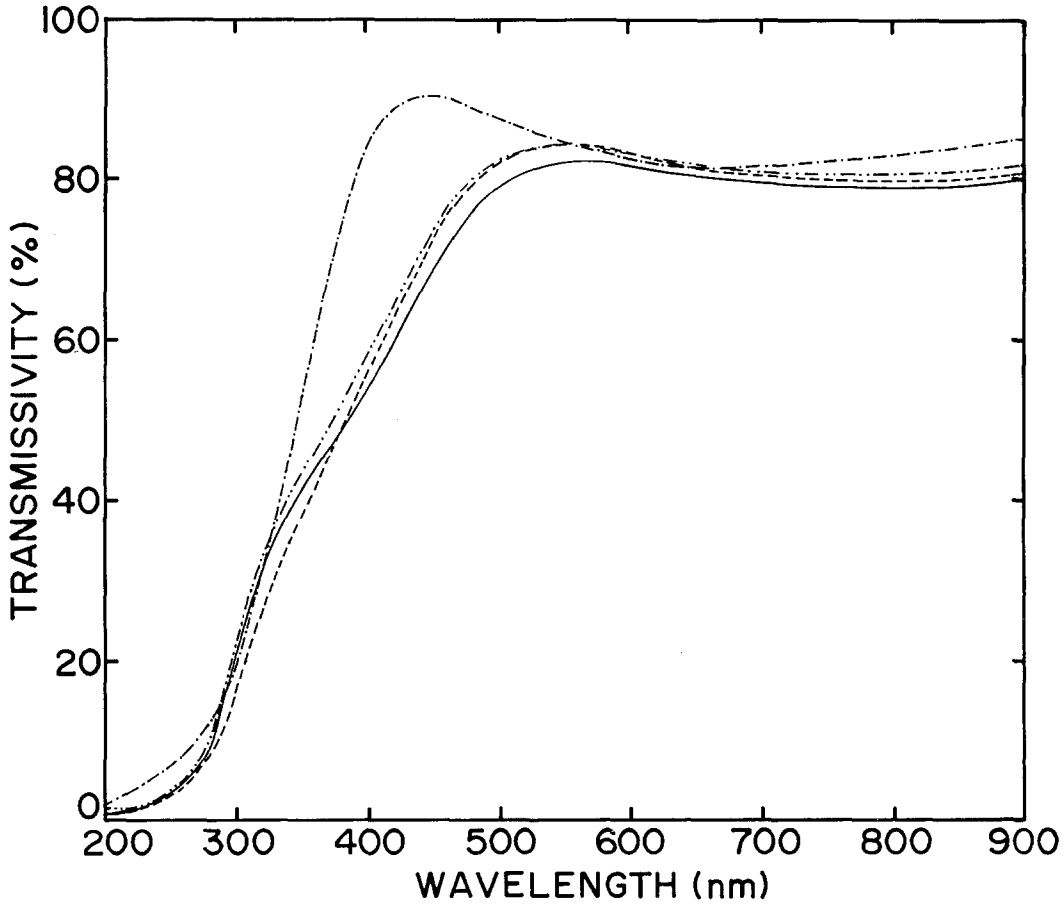

Figure 5 Transmissivity of as-deposited films: (——) Film (a), (—··—) Film (b), (– – –) Film (c), (—·—) Film (d). Film thickness is between 110 and 114 nm.

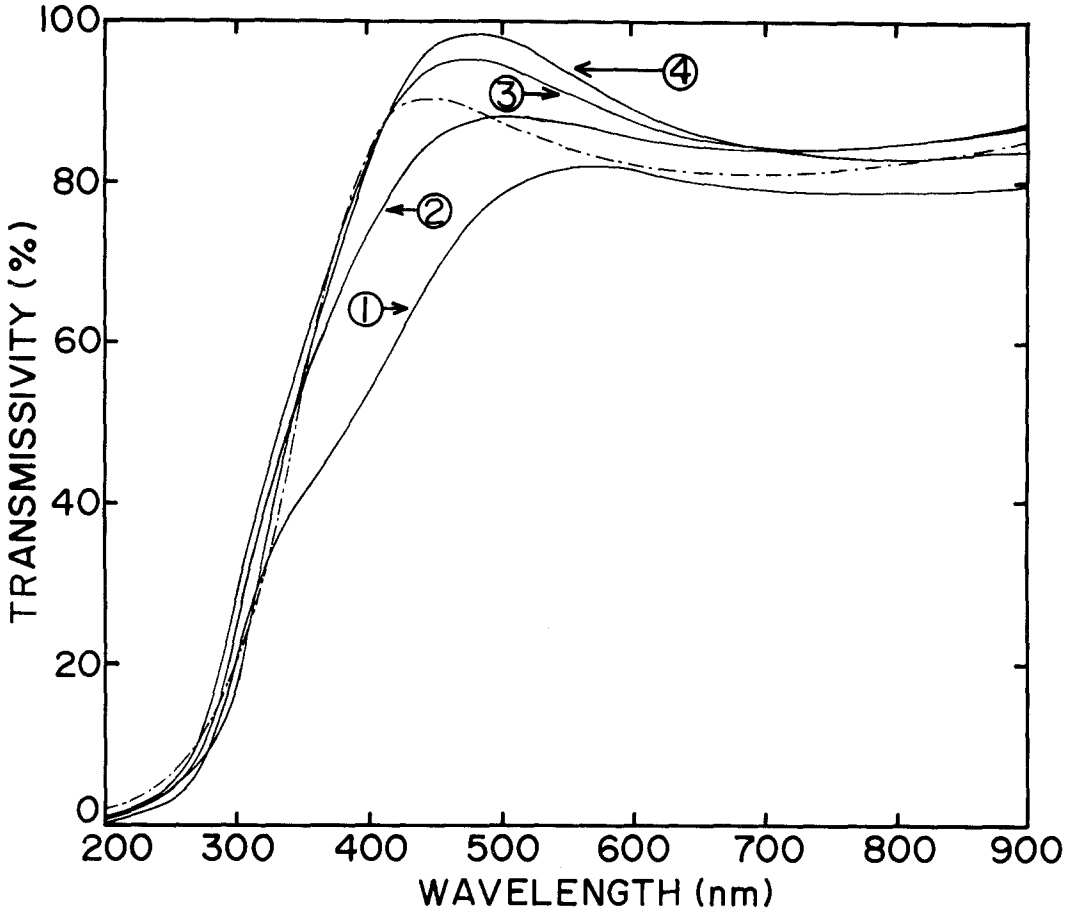

Figure 6 Effect of annealing on the transmissivity of the multilayered Film (a): (1) as-deposited, (2) annealed 300° C for 0.5 h, (3) 300° C for 5 h, (4) 500° C for 16 h.

annealing. Three features are obvious as the effects of annealing: first, the increased transmissivity of Film (a) centred around 480 nm; second, the higher transmissivity of Film (a) around 310 to 320 nm compared with Film (d); and finally the overall increase of transmissivity of Films (a), (b) and (c). These observations indicate that a higher visible transmissivity of the multilayered films could be achieved by the post-decomposition annealing of the films at higher temperatures. Thus, our next step is to examine the possibility of improving the electrical properties by annealing the multilayered films.

3.3. Electrical properties

Hall coefficient measurements were carried out at room temperature to determine the value of the carrier concentration n and the mobility μ_H. The measurements indicate that these multilayered films are n-type semiconductors. Fig. 7 shows the averaged resistivity ϱ of as-deposited and annealed films. A representative deviation from the averaged value is also given. As-deposited Films (a), (b) and (c) have almost the same resistivity of $\varrho = (1 \text{ to } 2) \times 10^{-3}\,\Omega\text{cm}$. Film (d) has a slightly larger resistivity of $\varrho = 3 \times 10^{-3}\,\Omega\text{cm}$. Post-deposition annealing has a large effect on the resistivity. Annealing of Films (c) and (d) always increases the resistivity, but the resistivity of Films (a) and (b) rather decreases except for annealing at 500° C for 16 h. The best result, $\varrho = 6 \times 10^{-4}\,\Omega\text{cm}$, is obtained in Film (b) when annealed at 300° C for 0.5 h. Generally, annealing at high temperatures to enhance the solid-solution formation decreases the resistivity. Figs 8 and 9 show the carrier concentration n and the Hall mobility μ_H, respectively. It is observed that the resistivity is largely dependent on the carrier concentration. The higher carrier concentration, $n = (5 \text{ to } 6) \times 10^{20}\,\text{cm}^{-3}$, is obtained in Films (a) and (b) when annealed at 300°C for 0.5 h. Annealing of

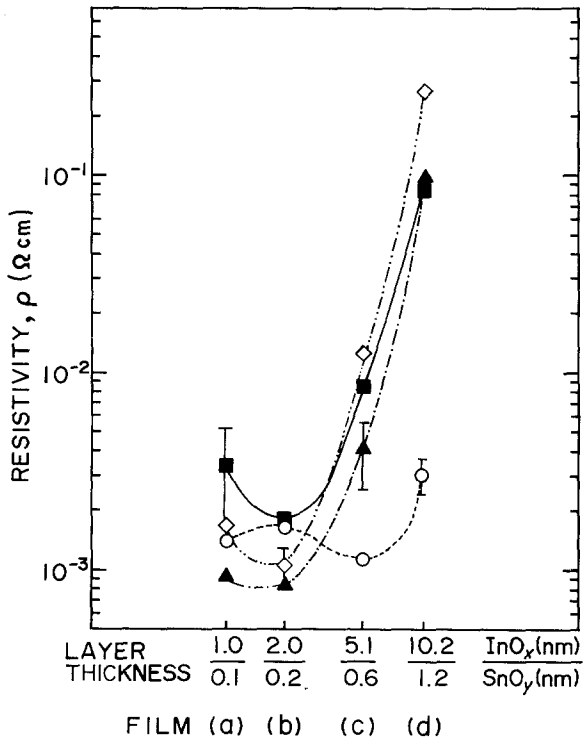

Figure 7 Effect of annealing on the resistivity of multilayered films: (○) as-deposited, (▲) 300° C for 0.5 h, (◇) 300° C for 5 h, (■) 500° C for 16 h.

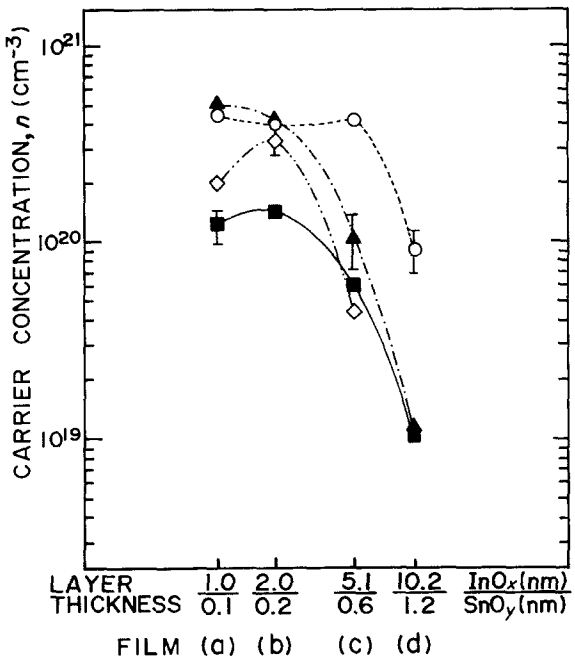

Figure 8 Effect of annealing on the carrier concentration (free electron density) of multilayered films: (○) as-deposited, (▲) 300° C for 0.5 h, (◇) 300° C for 5 h, (■) 500° C for 16 h.

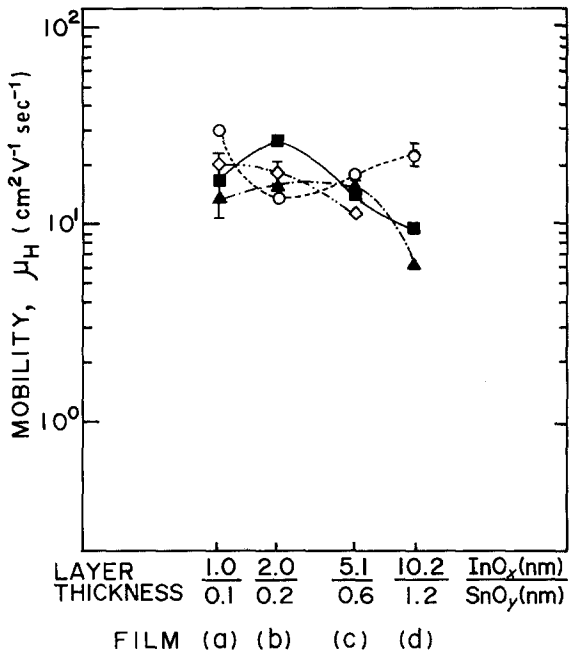

Figure 9 Effect of annealing on the Hall mobility of multilayered films: (○) as-deposited, (▲) 300° C for 0.5 h, (◇) 300° C for 5 h, (■) 500° C for 16 h.

Films (c) and (d) at 500° C remarkably reduced the carrier concentration down to the order of 10^{19} cm^{-3}. On the other hand, the Hall mobility does not change so markedly as the carrier concentration does. The Hall mobility remained almost in the range μ_H = 10 to 30 cm^2 V^{-1} sec^{-1}.

The largest difference in the electrical properties between the SnO_2-doped In_2O_3 solid solutions (ITO films) in the literature data and the multilayered films studied here seems to lie in the Hall mobility. Our best result is μ_H = 30 cm^2 V^{-1} sec^{-1}. Higher values in ITO films are often reported. For example, Ovadyahu *et al.* [5] prepared In_2O_{3-x} doped with tin by thermal evaporation and reported μ_H = 70 cm^2 V^{-1} sec^{-1}. Hamberg and Granqvist [2] showed that reactively evaporated tin-doped In_2O_3 films had μ_H = 77 to 79 cm^2 V^{-1} sec^{-1}.

So far as the electrical properties are concerned, annealing at 300° C for 0.5 h gives the best result; however, this condition is unfavourable for obtaining better optical properties. Further research on a variety of combinations of composition, layer thickness of multilayered films and post-deposition annealing is needed for achieving the optimum optoelectrical properties of ITO films.

4. Conclusions

1. Four kinds of multilayered films of indium oxide (InO_x)/tin oxide (SnO_y) were deposited on fused quartz substrates by ion-beam sputtering.

2. The layer thicknesses (in nanometres) of an InO_x/SnO_y pair and the pair numbers of four films were 1.0/0.1 × 100, 2.0/0.2 × 50, 5.1/0.6 × 20 and 10.2/1.2 × 10 pairs. The total thickness of the films was from 110 to 114 nm.

3. Low-angle X-ray diffraction analysis showed the formation of regular layered structures except for the film of 1.0/0.1 × 100 pairs.

4. As-deposited films of 5.1/0.6 × 20 pairs and 10.2/1.2 × 10 pairs were amorphous; however, the other two films showed broad peaks corresponding to the (2 2 2) and (4 0 0) planes of cubic In_2O_3.

5. Annealing at 500° C for 16 h still showed the existence of a periodic nature along the film thickness, except for the film of 100 pairs.

6. Annealing generally increased the visible transmissivity; however, the resistivity of films of 5.1/0.6 × 20 pairs and 10.2/1.2 × 10 pairs always increased with annealing. Hall effect measurements showed that the increase of resistivity was due to a reduction of the carrier concentration (free electron density).

7. The best visible transmissivity of about 90% was obtained in films of 1.0/0.1 × 100 pairs annealed at 500° C for 16 h. On the other hand, the lowest resistivity of 6 × 10^{-4} Ω cm was achieved on annealing the films of 2.0/0.2 × 50 pairs at 300° C for 0.5 h.

Acknowledgements

We thank Professor K. Fujibayashi of the Department of Electrical Engineering for supplying the electromagnet and Professor N. Oyama of the Department of Applied Chemistry for Resources for help in film thickness analysis.

References

1. K. L. CHOPRA, S. MAJOR and K. PANDYA, *Thin Solid Films* **102** (1983) 1.
2. I. HAMBERG and C. G. GRANQVIST, *J. Appl. Phys.* **60** (1986) R123.
3. T. SUZUKI, T. YAMAZAKI, H. YOSHIOKA, K. TAKAHASHI and T. KAGEYAMA, *J. Mater. Sci. Lett.* **6** (1987) 437.
4. T. SUZUKI, T. YAMAZAKI, K. TAKAHASHI, T. KAGEYAMA and H. ODA, *ibid.* **7** (1988) 79.
5. Z. OVADYAHU, B. OVRYN and H. W. KRANER, *J. Electrochem. Soc.* **130** (1983) 917.

Received 14 September
and accepted 10 December 1987